AAC Journals.ASM.org

Deletion of Tn*AbaR23* Results in both Expected and Unexpected Antibiogram Changes in a Multidrug-Resistant *Acinetobacter baumannii* Strain

Mandira Kochar,[a,d] Marialuisa Crosatti,[a] Ewan M. Harrison,[a] Barbara Rieck,[a] Jacqueline Chan,[e] Chrystala Constantinidou,[e] Mark Pallen,[e] Hong-Yu Ou,[b] and Kumar Rajakumar[a,c]

Department of Infection, Immunity and Inflammation, University of Leicester, Leicester, United Kingdom[a]; State Key Laboratory of Microbial Metabolism, Shanghai Jiao Tong University, Shanghai, China[b]; Department of Clinical Microbiology, University Hospitals of Leicester NHS Trust, Leicester, United Kingdom[c]; Centre for Mycorrhizal Research, Biotechnology and Management of Bioresources Division, The Energy and Resources Institute, Darbari Seth Block, India Habitat Centre, New Delhi, India[d]; and Centre for Systems Biology, School of Biosciences, University of Birmingham, Birmingham, United Kingdom[e]

Since the 2006 discovery of the *Acinetobacter baumannii* strain AYE AbaR1 resistance island, similar elements have been reported in numerous members of this species. As AbaR1 is distantly related to Tn*7*, we have renamed it Tn*AbaR1*. Tn*AbaR* transposons are known to carry multiple antibiotic resistance- and efflux-associated genes, although none have been experimentally studied *en bloc*. We deleted the Tn*AbaR* transposon in *A. baumannii* A424, which we have designated Tn*AbaR23*, and characterized independent deletion mutants DCO163 and DCO174. The NotI pulsed-field gel electrophoresis (PFGE) profile of strain DCO174 was consistent with targeted deletion of Tn*AbaR23* alone, but strain DCO163 apparently harbored a second large genomic deletion. Nevertheless, "subtractive amplification" targeting 52 Tn*AbaR* and/or resistance-associated loci yielded identical results for both mutants and highlighted genes lost relative to strain A424. PCR mapping and genome sequencing revealed the entire 48.3-kb sequence of Tn*AbaR23*. Consistent with Tn*AbaR23* carrying two copies of *sul1*, both mutants exhibited markedly increased susceptibility to sulfamethoxazole. In contrast, loss of *tetAR*(A) resulted in only a minor and variable increase in tetracycline susceptibility. Despite not exhibiting a growth handicap, strain DCO163 was more susceptible than strain DCO174 to 9 of 10 antibiotics associated with mutant-to-mutant variation in susceptibility, suggesting impairment of an undefined resistance-associated function. Remarkably, despite all three strains sharing identical *gyrA* and *parC* sequences, the ciprofloxacin MIC of DCO174 was >8-fold that of DCO163 and A424, suggesting a possible paradoxical role for Tn*AbaR23* in promoting sensitivity to ciprofloxacin. This study highlights the importance of experimental scrutiny and challenges the assumption that resistance phenotypes can reliably be predicted from genotypes alone.

The clinical significance of *Acinetobacter baumannii* has grown substantially over the last few decades largely due to the fact that this species possesses an extensive repertoire of innate antimicrobial resistance mechanisms and a remarkable capacity to acquire and express a diverse range of foreign resistance determinants. Whole-genome sequence analysis of *A. baumannii* is providing valuable insights into the genetic complexity and genomic agility of this pathogen and has also revealed extensive strain-to-strain variation in the repertoires of known and putative resistance-associated genes.

Over the last 4 years, it has been increasingly recognized that many *A. baumannii* strains possess highly clustered assemblages of resistance genes and associated mobile elements mapping to genomic segments that are closely related to AbaR1, an ~86-kb element found in *A. baumannii* strain AYE which was predicted to encode resistance via 45 genes to several heavy metals and multiple classes of antimicrobial agents (14). This single, potentially mobile element, through diverse genes which have probably been acquired from several bacterial genera, is predicted to encode resistance to β-lactams, aminoglycosides, chloramphenicol, rifampin, tetracyclines, sulfonamides, and several heavy metals (2, 14). This resistance island type architecture also provides the perfect storehouse for class 1 integrons, insertion sequences, and transposons, thus aiding the transfer of drug resistance determinants (14).

Increasing numbers of AbaR1-like resistance islands have been identified in the last 2 years. These have been numbered consecutively and include at least 20 members identified in *A. baumannii* strains belonging to the European clone I lineage (1, 2, 18, 19, 24, 25). In addition, AbaR2 from *A. baumannii* ACICU, a likely remnant of an AbaR1-like element, was until recently the only such element found in a European clone II strain to have been characterized (17).

A feature common to all but one of the characterized AbaR1-like elements is that these elements disrupt the *comM* gene, which codes for a predicted competence-associated protein, in a site-specific manner. The *comM* gene also serves as an integration hot spot, though much less frequently, for several other evolutionarily distinct, horizontally acquired DNA sequences (2, 14, 29). PCR interrogation of the *comM* locus in 52 genotypically diverse multidrug-resistant *A. baumannii* clinical isolates suggested a *comM*-associated AbaR1-like carriage rate of ~65% in this species (M.

Received 20 July 2011 **Returned for modification** 1 September 2011
Accepted 15 January 2012
Published ahead of print 30 January 2012
Address correspondence to Kumar Rajakumar, kr46@le.ac.uk.
M.K. and M.C. contributed equally to this article.
Supplemental material for this article may be found at http://aac.asm.org/.

doi:10.1128/AAC.05334-11

TABLE 1 Bacterial strains and plasmids used in this study

Bacterial strain or plasmid	Description, genotype, or relevant characteristics[a]	Reference or source
Acinetobacter baumannii strains		
AYE	Epidemic MDR type strain	14
AB0057	MDR type strain	2
ATCC 19606	Type strain	Salmonella Genetic Stock Centre
ACICU	Epidemic MDR type strain	17
A424	Clinical isolate from Croatia	Kevin Towner
A424ΔTn*AbaR23*-163	A424 derivative with Tn*AbaR23* deleted plus an additional genomic deletion and/or rearrangement	This study
A424ΔTn*AbaR23*-174	A424 derivative with Tn*AbaR23* deleted	This study
Escherichia coli strains		
DH5α	F$^-$ *ϕ*80d*lacZ*ΔM15 Δ(*lacZYA-argF*)*U169 deoR recA1 endA1 hsdR17*(r_K^- m_K^+) *phoA supE44* λ$^-$ *thi-1*	Lab stock
CC118λ*pir*	Δ(*ara-leu*) *araD* Δ*lacX74 galE galK phoA thi-1 rpsE rpoB argE*(Am) *recA1*; lysogenized with λ*pir* phage	16
S17.1λ*pir*	*hsdR recA pro* RP4-2 (Tc::Mu; Km::Tn*7*)(λ*pir*)	12
Plasmids		
pJTOOL-3	Derivative of suicide vector pDS132; R6K *ori mob*RP4 *sacB*; Cm^r	32
pJTAG	pJTOOL-3 derivative carrying the SOE-PCR product of Tn*AbaR1* UF–*aacC1*–Tn*AbaR1* DF; Cm^r Gm^r	This study

[a] Abbreviations: MDR, multidrug resistant; Cm^r, chloramphenicol resistance; Gm^r, gentamicin resistance.

Kochar and K. Rajakumar, unpublished data). Critically, detailed bioinformatic analyses of the termini of AbaR1-like elements across multiple *A. baumannii* strains has provided the strongest evidence yet that these elements have arisen from an ancestral Tn*7*-like transposon. Accordingly, we have renamed AbaR1 Tn*AbaR1* and extended this nomenclature to the wider family of these elements (27). In all likelihood, the ancestral Tn*AbaR* transposon diversified through acquisition, often in a nested fashion, of a large variety of transposons, integrons, and resistance gene cassettes, supplemented by deletions, duplications, rearrangements and/or the acquisition of point mutations. Tn*AbaR* transposons carry genes predicted to code for resistance to a wide range of antibiotics and several efflux-associated systems. The latter include likely representatives of resistance-nodulation-division (RND), major facilitator superfamily (MFS), multidrug and toxic compound extrusion (MATE), and small multidrug resistance (SMR) transporter superfamilies, other examples of which have been shown to contribute to resistance in *A. baumannii* (11, 31, 33).

In this study, we have deleted *en bloc* the Tn*AbaR* transposon in *A. baumannii* strain A424 (Tn*AbaR23*) and performed resistance testing and genetic characterization of two independent Tn*AbaR*-minus mutants and the wild-type parent to gain insight into the phenotypic contribution of this element. *A. baumannii* A424 was originally isolated from a case of invasive infection in Croatia. We propose that this large-scale genomic deletion approach could facilitate systematic analyses of resistance in *Acinetobacter* and provide phenotypic profiles for Tn*AbaR* elements and other resistance-associated assemblages.

MATERIALS AND METHODS

Bacterial strains, plasmids, and media. Details of bacterial strains and plasmids used in this study are listed in Table 1. *A. baumannii* strain A424, provided by Kevin Towner, Queen's Medical Centre, Nottingham, United Kingdom, was originally isolated from a patient in Croatia with an invasive infection. All strains were grown at 37°C at 200 rpm in Luria-Bertani (LB) medium, except for selection of *A. baumannii* merodiploids which was performed on Simmons citrate agar (Oxoid, Basingstoke, United Kingdom) (13). Gentamicin (20 μg/ml or 100 μg/ml) and chloramphenicol (20 μg/ml) were added as required.

DNA analysis and manipulation procedures. Genomic and plasmid DNA purification, enzymatic manipulation of DNA, other routine recombinant DNA technology methods, and pulsed-field gel electrophoresis (PFGE) experiments were performed according to previously described protocols (15, 26). *A. baumannii* strain A424 was sequenced by 454 GS FLX pyrosequencing (Roche, Branford, CT) according to the standard protocol for whole-genome shotgun sequencing and assembled using the xBASE *de novo* assembly pipeline (9) and Newbler 2.5 (Roche). pJTAG was constructed by amplifying ~750 to 800 bp of sequence in the regions immediately upstream and downstream of Tn*AbaR1* in strain AYE using the primer pairs AbaRUF/AbaRURGm (Gm stands for gentamicin) and AbaRDFGm/AbaRDR, respectively (see Fig. S1 in the supplemental material). These fragments were joined by splicing overlap extension (SOE) PCR to a Flippase recognition target (FRT)-flanked *aacC1* cassette amplified with primers GmF (F stands for forward) and GmR (R stands for reverse) from pUC18T-mini-Tn*7*T-Gm (10). KOD Hot Start DNA polymerase (Novagen, Merck Biosciences, United Kingdom) was used according to the manufacturer's instructions for the SOE-PCR protocol. The resulting 2.7-kb SOE PCR product was restricted with NotI and cloned into the pDS132-derived suicide vector pJTOOL-3 using the *Escherichia coli* CC118λ*pir* host (16, 32). The resultant plasmid, pJTAG, was transferred into *E. coli* S17.1λ*pir* (12) and then conjugally mobilized into *A. baumannii* strain A424 (Fig. S1). Details of primers used in this study are shown in Table S1 in the supplemental material.

Construction of Tn*AbaR23*-minus mutants by conjugative delivery of pJTAG. Overnight cultures of the recipient *A. baumannii* A424 and the donor *E. coli* S17.1λ*pir*/pJTAG were subcultured into antibiotic-free medium and grown to mid-log phase. The cells were pelleted, resuspended in 1 ml prewarmed LB medium, combined in a 1:1 ratio, and then centrifuged at low speed at room temperature. The supernatant was discarded, and the cells were resuspended in 50 μl of 10% glycerol and spotted onto the center of a nonselective LB agar plate. This mating plate was left overnight at 37°C, and the cells were then scraped off and resuspended in 400 μl of 10% glycerol; appropriate dilutions were plated onto Simmons citrate agar supplemented with gentamicin (100 μg/ml). Putative merodiploid derivatives were maintained on LB agar supplemented with gentamicin (100 μg/ml), verified by PCR analysis, plated at high density onto LB

agar supplemented with 6% sucrose, and incubated at 37°C for counterselection of the pJTOOL-3-borne *sacB* (32).

Antimicrobial susceptibility testing and MIC determination. Iso-Sensitest agar (Oxoid, Basingstoke, United Kingdom) was used for disc diffusion susceptibility and Etest-based MIC assays which were performed according to British Society for Antimicrobial Chemotherapy (BSAC) guidelines (3). All results shown are based on a minimum of three replicates. Antibiotic discs were purchased from Oxoid (Basingstoke, United Kingdom), while Etest strips were obtained from AB Biodisk (Solna, Sweden).

Nucleotide sequence accession number. The sequence of Tn*AbaR23* of *A. baumannii* strain A424 has been deposited in GenBank under accession number JN676148.

RESULTS AND DISCUSSION

Targeted *en bloc* deletion of the Tn*AbaR23* transposon from *Acinetobacter baumannii* strain A424. PCR analysis of the multiantibiotic-resistant *A. baumannii* strain A424 using primer pairs 2F/2R and 4F/4R which targeted the well-conserved *comM*-Tn*AbaR* junctions (29) demonstrated that A424 harbored a typical Tn*AbaR*-like transposon in the *comM* gene. This element was designated Tn*AbaR23*. A pDS132-based suicide plasmid, pJTAG, carrying the characteristic Tn*AbaR*-flanking 5′ and 3′ *comM*-associated targeting sequences interrupted by an *aacC1* gentamicin resistance-encoding cassette, was introduced into strain A424 by conjugation (see Fig. S1 in the supplemental material). Two independent single-crossover mutants were then subjected to a sucrose selection step to identify likely double-crossover mutants that had lost the entire Tn*AbaR* transposon. Candidate double-crossover mutants were analyzed by PCR using primers AbaRUF2 and AbaRDR2 that anneal to regions just outside those on the pJTAG targeting sequences (Fig. S1). Two Tn*AbaR* deletant mutants, A424ΔTn*AbaR23*-163 (DCO163) and A424ΔTn*AbaR23*-174 (DCO174), each derived from an independent single-crossover mutant, were identified by the production of an expected 3.7-kb amplicon. As predicted, no amplicons were produced for strains A424 and AYE, while strain ATCC 19606, which harbors an uninterrupted *comM* gene, yielded an expected 2.5-kb product (Fig. 1A). The deleted *comM*-borne transposon in strain A424 has henceforth been referred to as Tn*AbaR23*.

High-molecular-weight DNA purified from strain A424 and its Tn*AbaR23*-minus isogenic mutants, DCO163 and DCO174, was digested separately with NotI and SfiI and examined by PFGE analysis (Fig. 1B). Despite both mutants being constructed identically and being confirmed to be indistinguishable from strain A424 by analysis of six sequence-polymorphic *A. baumannii* genes (*ABAYE3778*, *filE*, *ompA*, *lldD*, *ABAYE3780*, and *filB*), both the NotI and SfiI profiles of DCO163 and DCO174 exhibited minor band discrepancies. The NotI banding patterns of A424 and DCO174 were consistent with targeted deletion of Tn*AbaR23* alone (Fig. 1B), while that of DCO163 could be explained only by a further genomic rearrangement event, potentially triggered by conjugation and/or allelic exchange. Indeed, based on summation of the observed DCO163 NotI fragments, it would appear that this strain had lost a further ~50 kb of DNA by comparison with DCO174. Nevertheless, it should be noted that despite repeated subculture, PFGE genomic profiles of the two mutants have remained unchanged from those detected originally, strongly supporting the notion that the described genome configurations are stable and not prone to further spontaneous undefined genome rearrangements.

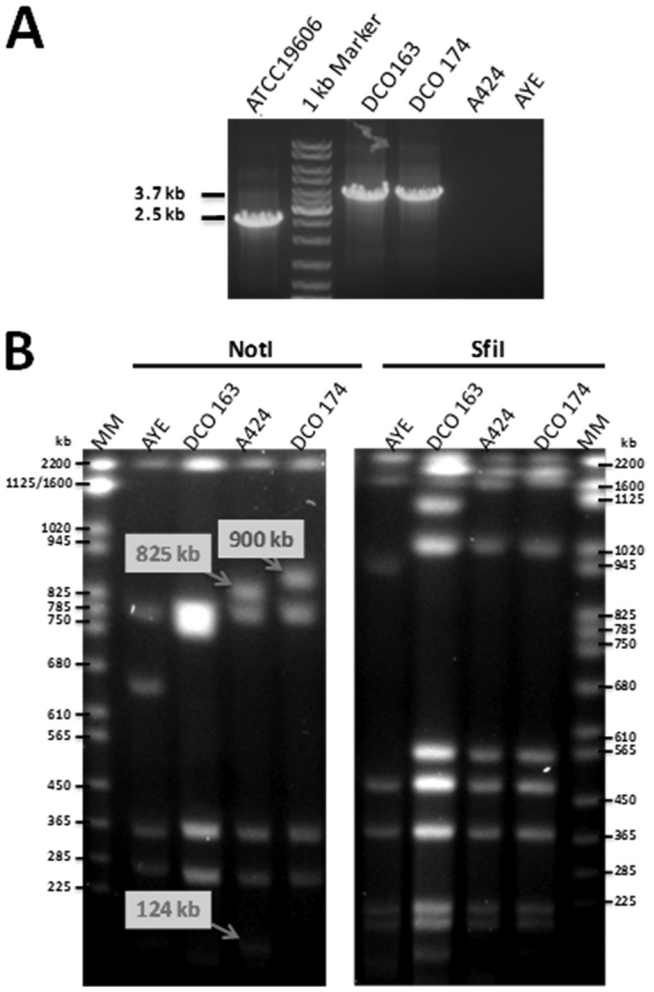

FIG 1 Analysis of the putative Tn*AbaR23*-minus mutants of *Acinetobacter baumannii* A424. (A) PCR amplification across the targeted deleted locus in DCO163 and DCO174 mutant strains using the primers AbaRUF2 and AbaRDR2 yielded the expected ~3.7-kb product, while failing to amplify across the A424 Tn*AbaR23* element. The sequenced strains ATCC 19606 and AYE that lacked and harbored an island within the *comM* gene were used as positive (2.5-kb band expected) and negative PCR controls, respectively. (B) Pulsed-field gel electrophoresis analysis of NotI- and SfiI-digested A424, DCO163, DCO174, and AYE high-molecular-weight genomic DNA. The three bands with arrows and labels indicate the only observed NotI profile differences between A424 and DCO174. Subsequently available sequence data showed that Tn*AbaR23* harbors two very closely spaced NotI sites, while the replacement cassette lacks a NotI site. Hence, the observed loss of two A424 bands (825 kb plus 124 kb) and the appearance of a new DCO174-specific band (900 kb), with the difference between the two being the size of Tn*AbaR23* (48.3 kb). Lanes MM contain molecular size markers.

Use of a novel combined subtractive amplification-PCR mapping strategy to define the genetic composition and organization of Tn*AbaR23*. PCR primer pairs targeting 52 genes/loci selected empirically from those found within Tn*AbaR3* to Tn*AbaR4* and/or associated directly with resistance in *A. baumannii* were designed. The parent strain A424 and its Tn*AbaR23* deletant derivatives were subjected to PCR assays specific to each of these targets. Examination of this "subtractive amplification" data set allowed for firm conclusions as to genes/loci that mapped specifically to Tn*AbaR23* (see Table S2 in the supplemental material).

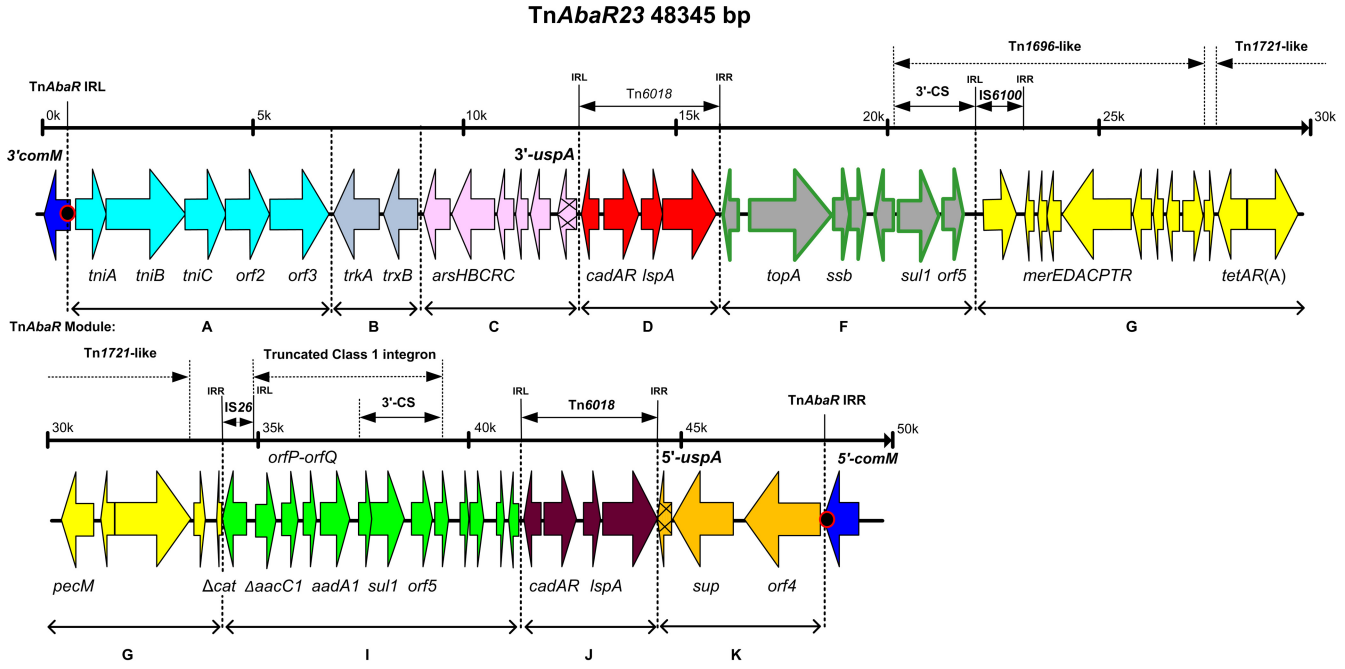

Repeat	Type	Sequence 5' to 3'
IS*26* IRL / IRR	Inverted	GGCACTGTTGCAAA
IS*6100* IRL / IRR	Inverted	GGCTCTGTTGCAAA
Tn*6018* IRL	Inverted	GGGTAAGCGGATTAAATGGTTGAT
Tn*6018* IRR	Inverted	GGGTATACGGATTTAATGGTTGAT
Tn*AbaR* IRL	Inverted	TGTCATTTACAGCAATAGAATAGAGT
Tn*AbaR* IRR	Inverted	TGTCAGTTCCACAAATAAATCAGAGT

FIG 2 Schematic map showing the genetic organization of Tn*AbaR23*. Genes are colored by module (see Fig. 3 for details) with key genes labeled. The locations of identified repeat sequences (inverted repeat left [IRL] and inverted repeat right [IRR]) are indicated (positions are shown in thousands[k] from 0k to 50k), and full sequence details are shown in the graph at the bottom of the figure. The red circles shown at both Tn*AbaR23* ends indicate the 5-bp direct repeat sequences (5′-ACCGC-3′) which flank this element. Study-defined module boundaries are shown as dotted lines (see text and the legend to Fig. 3 for details). This figure is drawn to scale. Full annotation details for Tn*AbaR23* are available in GenBank (accession number JN676148). Minor annotation changes represented in this figure are listed in Table S4 in the supplemental material. 3′-CS, 3′ conserved sequence.

A series of conventional short- and long-range PCR mapping assays informed by these gene content data and the recognized organization of previously characterized Tn*AbaR* elements were then performed to completely map Tn*AbaR23* (Table S3). Whole-genome sequencing of strain A424 yielded ~120,000 reads with an average length of 450 bp. Almost all (97.7%) of the reads were aligned into 715 contigs with a peak depth of eight and an estimated genome size of ~3.9 Mb. These data have been submitted to the Sequence Read Archive under accession number SRA045827.2. Further examination of the contigs allowed definition of the entire 48.3-kb sequence of Tn*AbaR23* (GenBank accession number JN676148) (Fig. 2).

Genetic organization of Tn*AbaR23* and modular mosaicism of Tn*AbaR* transposons. The genetic organization and modular composition of Tn*AbaR23* were systematically defined through comparative genomic analysis against 15 other Tn*AbaR* elements chosen empirically to represent major known variants. For consistency, we used broad module definitions previously proposed by Adams et al. (2) who compared five Tn*AbaR* islands (Tn*AbaR0* to Tn*AbaR4*) in four *A. baumannii* strains but refined these to define precise module boundaries based on the *TnAbaR1* sequence and other secondary reference sequences where necessary. One each of a Tn*AbaR2*-specific insert and a Tn*AbaR4*-specific insert previously identified by Adams et al. (2) and an additional two Tn*AbaR*-associated segments have now been assigned module names and included in our updated comparative schematic (Fig. 3). Based on identification of repeat sequences, four modules (D, J, L, and N) undoubtedly represented genuine genetic modules, while all others have been inferred solely by comparative means. We emphasize that the modules we describe are a reflection of the set of sequences compared and the original Adams et al. (2) module definitions and that these do not necessarily reflect individual genetic units. Indeed, a Tn*1696*-like unit is found to span adjacent modules E and G in Tn*AbaR1* and modules F and G in eight of the other elements analyzed. While the modular schema we have presented offer the advantage of simplicity and intuitive interpretation, particularly when analyzing large numbers of genome sequences, we direct interested readers to detailed studies pioneered by Post et al. (24) and subsequently extended by others that have attempted to deconstruct Tn*AbaR* elements through precise identification and definition of boundaries of transposon-, IS element-, and integron-related sequences (1, 18, 19, 25). We have captured some but not all of these finer-level data in Fig. 2 and 3. Furthermore, based on the hypothesized path of evolution of Tn*AbaR* transposons proposed by Post et al. (25), modules C and K would have been contiguous in an ancestral

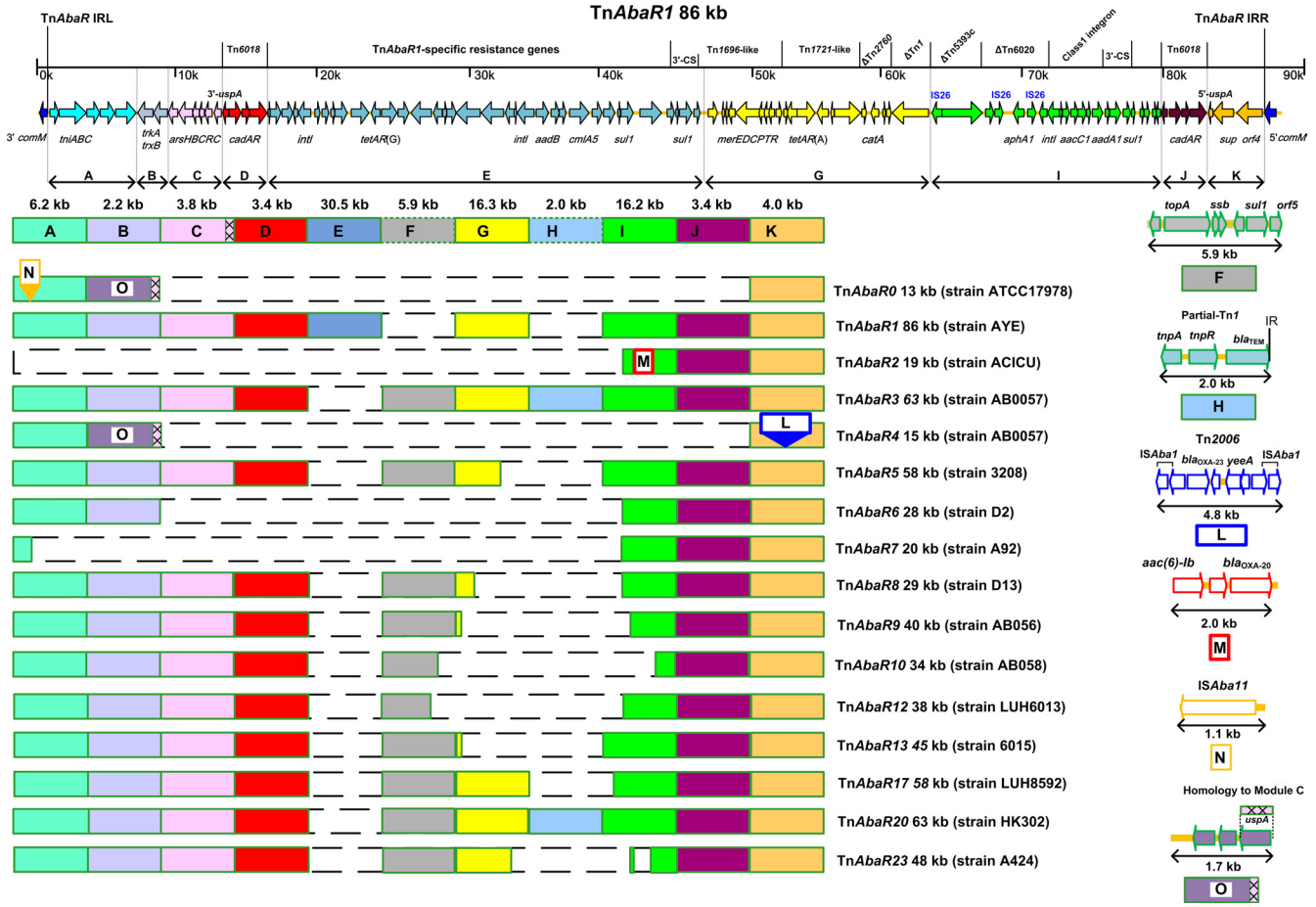

FIG 3 Comparison of the modular compositions of 15 previously characterized *A. baumannii* Tn*AbaR* transposons and that of Tn*AbaR23*. A schematic representation of Tn*AbaR1* drawn to scale with genes colored by module and module boundaries as indicated is shown in the map at the top of the figure; selected genes are labeled. Details of six further modules not represented within Tn*AbaR1* are shown below the map to the right. Full annotation details of Tn*AbaR1* and the remaining modules are available via GenBank; accession numbers are listed below or in Table S5 in the supplemental material. Minor annotation changes represented in this figure are listed in Table S4. Modules A to K are shown as equal-sized rectangles when intact or as terminally or internally truncated boxes, as appropriate, to highlight incomplete modules. Rectangles outlined by large dashes represent deleted and/or absent modules. Modules N and L are inserted at sites as shown, while module M in Tn*AbaR2* occurs in place of a part of module I. Module O is restricted to Tn*AbaR0* (previously designated Tn*6021*) and Tn*AbaR4* and possess an ~500-bp segment that exhibits high-level identity to a matching segment of the highly conserved module C; corresponding homologous sequences are shown crosshatched. The size to the nearest kilobase and host strain information are as shown. Tn*AbaR4* is the only characterized member of this family which is not inserted into the *comM* gene. Additional genetic features are shown where particularly pertinent. The Tn*AbaR* transposons shown above and the GenBank accession numbers of the transposons or associated genomes (shown in parentheses) are as follows: Tn*AbaR0* (CP000521), Tn*AbaR1* (CT025832), Tn*AbaR2* (CP000863), Tn*AbaR3* (CP001182), Tn*AbaR4* (CP001182), Tn*AbaR5* (FJ172370), Tn*AbaR6* (GQ406245), Tn*AbaR7* (GQ406246), Tn*AbaR8* (HM590877), Tn*AbaR9* (project accession ADGZ01000000), Tn*AbaR10* (project accession ADHA01000000), Tn*AbaR12* (JF262168), Tn*AbaR13* (JF262169), Tn*AbaR17* (JF262173), Tn*AbaR20* (HM357806), and Tn*AbaR23* (JN676148).

transposon, designated Tn*6019* by Post et al. Separation of modules C and K was proposed to have followed insertion of a Tn*6018*-flanked compound transposon into *uspA*. Intriguingly, all seven European clone II strains studied by Post et al. (25) possessed an intact *uspA* gene, while the reverse was true for all known European clone I strains, perhaps with the exception of Tn*AbaR4*. Tn*AbaR23*, like most defined Tn*AbaR* elements possesses intact versions of the terminal modules A and K. The former carries the left terminal inverted repeat and the *tniA-tniB-tniC-orf2-orf3* tandem cluster (previously designated *orf1-tniA-tniB-orf2-orf3* [27]), members of which show protein-level homology to Tn*7* transposition-associated partners and/or are postulated to partake in transposition (27), while the latter carries the cognate right terminal inverted repeat. Hence, like most other elements in this family, Tn*AbaR23* would appear to possess the genetic machinery required for active transposition. In contrast, Tn*AbaR2* in strain ACICU appears to have arisen from a one-ended deletion that has led to the total loss of its transposition module, while Tn*AbaR7* retains only a short fossil remnant of module A which carries an intact *tniA* gene alone (Fig. 3).

In common with most other characterized Tn*AbaR* elements, Tn*AbaR23* also carries intact versions of modules B, C, D, F, and J, where modules D and J comprise one each of two directly orientated Tn*6018* elements (commonly designated IS*Ppu12*), at least one copy of which can be found in all but Tn*AbaR0* and the sole characterized non-*comM*-resident member of this family, Tn*AbaR4* (Fig. 3). Compared with Tn*AbaR1* and Tn*AbaR3*, the first two well-described members of this family, Tn*AbaR23* lacks

module E and module H. Module E is a 30.6-kb Tn*AbaR1*-specific segment that contains 20 resistance genes and components of three distinct class 1 integrons, while module H is a 2.0-kb bla_{TEM}-bearing truncated version of Tn*1* unique to Tn*AbaR3* (4). In addition, Tn*AbaR23* contains substantially truncated versions of modules G and I, two frequently contiguous resistance gene-bearing modules. Importantly, the Tn*AbaR23* module I remnant lacks a class 1 integron-associated *intI1* gene and an intact *attI1* site but contains a truncated *aacC1* proximal cassette that abuts onto an IS*26* element and at least two other resistance cassettes. The IS*26* element may have also contributed to the partial deletion of a second resistance gene as it adjoins on the other flank the 126-bp 3′ remnant of *cat* (Fig. 2).

In addition to the classical resistance genes identified on Tn*AbaR23* [*sul1*, Δ*aacC1*, *aadA1*, *tetAR*(A), and Δ*catA*], this element carries genes that code for components of several putative or likely efflux systems that could contribute toward the wider resistance phenotype of strain A424. These include the five-gene *arsCRCBH* operon that is predicted to confer resistance to arsenic and antimony and the cadmium resistance-associated Tn*6018*-borne *cadAR* genes (8, 28, 35). ArsB serves as an antiporter which effluxes arsenite ions (6, 23), while *cadA* and *cadR* code for a putative heavy metal-associated cation efflux transporter and a heavy metal resistance regulator (21), respectively. CadR contains a characteristic N-terminal helix-turn-helix domain and belongs to the PbrR transcription regulator family that also includes CadR of *Pseudomonas aeruginosa* and PbrR of *Ralstonia metallidurans* that regulate the expression of cognate cadmium and lead resistance operons, respectively. These latter proteins share an N-terminal DNA binding domain with other transcription regulators of the MerR superfamily (5, 7, 21). Module G carries the Tn*1696 merEDACPTR* gene cluster which codes for resistance to mercury (24). Based on similarities to Tn*21* counterparts, MerA is predicted to function as a mercuric reductase, while MerE and MerT (inner membrane proteins) and MerP (periplasmic protein) are hypothesized to constitute key structural components of the mercury transport system itself (30). The 4.0-kb module K carries the annotated genes *sup* and *orf4* and the 5′ remnant of *uspA*. Orf4 is an *A. baumannii*-specific uncharacterized protein, while Sup is a predicted MFS superfamily sulfate permease that exhibits either 100% identity or ~89% identity to counterparts encoded by all other Tn*AbaR* elements. Sup also bears striking homology with many other MFS family putative sulfate permeases from a wide range of bacteria. In addition, given that *topA* and *ssb* code for a predicted topoisomerase and single-stranded DNA binding protein, respectively, and that gyrase A and topoisomerase IV are known to interact with fluoroquinolones (20, 22), it would be intriguing if the Tn*AbaR23 topA* and/or *ssb* genes contributed to the unusual ciprofloxacin-associated high-level resistance phenotype observed in mutant strain DCO174 following deletion of Tn*AbaR23* (details below).

As shown in Fig. 3, Tn*AbaR1* at ~86 kb in size and with 45 likely resistance genes remains the largest Tn*AbaR* element identified thus far. At the other extreme, the ~13-kb Tn*AbaR* element found in strain ATCC 17978, which had originally been isolated in the 1950s, contains only one likely resistance-associated gene, *sup*. Based on these and previous comparative genomics data and our hypothesis regarding the core Tn*AbaR* components required for transposition (27), the ATCC17978 element almost certainly comprises or closely resembles the ancestral prototype of the

TABLE 2 Antimicrobial susceptibility of *Acinetobacter baumannii* strain A424 and its Tn*AbaR23*-minus mutants

Strain	Zone of inhibition diam (MIC) of strain to the following antibiotic[a]:														
	TET (10 μg)	IMP[c] (10 μg)	CAR (100 μg)	AMP (25 μg)	TIM (75 μg)	CTX (30 μg)	CIP[c] (5 μg)	STR (10 μg)	TOB (10 μg)	AMK (30 μg)	GEN[c] (10 μg)	TMP (2.5 μg)	SUL (25 μg)	SXT (25 μg)	CHL (10 μg)	RIF (2 μg)
AYE[b]	6.0	28.0 (0.38)	6.0	6.0	6.0	6.0 (>256)	**6.5 (>32)**	9.0	13.0	17.0	**8.5 (16)**	6.0	6.0 (>1,024)	6.0	6.0	6.0
A424	6.0	15.0 (4)	6.0	6.0	6.0	6.0 (>256)	**14.0 (4)**	16.0	26.0	16.0 (12)	23.0 (0.75)	6.5	6.0 (>1,024)	6.0	6.0	11.5
DCO163	15.0	18.0 (2)	6.0	6.0	6.0	6.0 (>256)	**16.0 (3)**	11.0	23.0	11.0 (48)	**9.0 (16)**	10.0	31.0 (0.75)	30.5	6.0	11.5
DCO174	9.5	15.0 (4)	6.0	6.0	6.0	6.0 (>256)	**6.0 (>32)**	9.0	23.0	9.0 (96)	**6.0 (48)**	6.0	23.5 (4)	21.5	6.0	13.0
NCTC12241[b]	20.0	35.0	18.0	13.0	NA	35.0	30.0	17.0	21.0	24.0 (1.5)	23.0	26.0	6.0 (>1,024)	29.0	20.0	6.0

[a] Antibiotic abbreviations: TET, tetracycline; IMP, imipenem; CAR, carbenicillin; AMP, ampicillin; TIM, ticarcillin-clavulanate; CTX, cefotaxime; CIP, ciprofloxacin; STR, streptomycin; TOB, tobramycin; AMK, amikacin; GEN, gentamicin; TMP, trimethoprim; SUL, sulfamethoxazole; SXT, sulfamethoxazole-trimethoprim; CHL, chloramphenicol; RIF, rifampin. The mass of antibiotic is given in parentheses after the antibiotic. NA, not available.

[b] AYE data were in accordance with previously published resistance data (Adams et al. [2] and references cited therein). *E. coli* strain NCTC12241 was used as a BSAC reference control.

[c] BSAC guidelines (3) on zone diameter breakpoints were as follows: for IMP, resistant (R) ≤ 13 mm, susceptible (S) ≥ 25 mm, and intermediate (I) = 14 to 24 mm; for CIP, R ≤ 20 mm and S ≥ 21 mm. BSAC (3) guidelines on MIC breakpoints for *Acinetobacter* species: for GEN, R > 4 mg/liter and S ≤ 4 mg/liter; for CIP, R > 1 mg/liter and S ≤ 1 mg/liter; for IMP, R > 8 mg/liter, S ≤ 2 mg/liter, and I = 4 to 8 mg/liter. Numbers shown in boldface type and underlined indicate resistant and intermediate, respectively, by BSAC interpretive criteria. MIC was tested using Etest strips (AB bioMérieux, Sweden), and the MIC results for antibiotics tested are shown in parentheses in the table. Each assay was repeated at least three times. Zone diameters are shown to the nearest 0.5 mm, while MIC is shown in milligrams per liter.

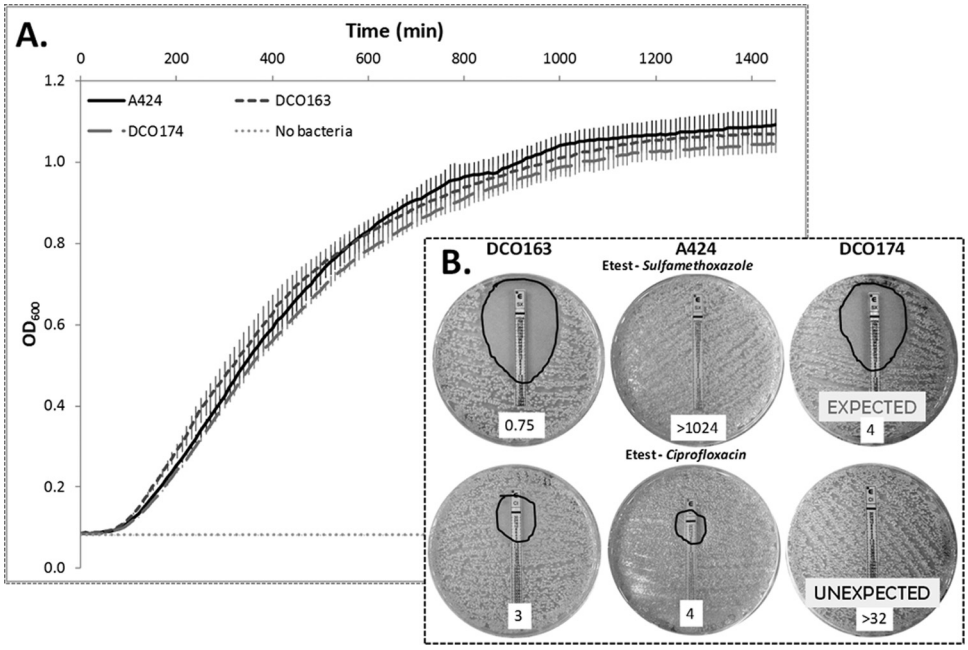

FIG 4 Growth curve and Etest analyses of *Acinetobacter baumannii* A424 and its Tn*AbaR23*-minus mutants. (A) The wild-type strain A424 and DCO163 and DCO174 mutants were grown in 200 μl antibiotic-free LB medium at 37°C with shaking in 96-well plates from standardized overnight cultures and monitored in a Multiskan GO instrument to determine the optical density at 600 nm (OD_{600}) measurements at 10-min intervals. The data shown represent the mean values ± standard deviations (error bars) for four independent wells for each strain. No significant difference in growth dynamics of the strains was observed. (B) Images of Etest assays for sulfamethoxazole and ciprofloxacin MICs on A424, DCO163, and DCO174 to highlight both an expected and an unexpected resistance phenotype of DCO174 associated with the loss of Tn*AbaR23*. The edges of the zones of inhibition have been outlined, and the measured MIC values (in micrograms per milliliter) are shown on the white labels at the bottom of the plate image. The switch to sulfamethoxazole susceptibility observed in both DCO163 and DCO174 was entirely predictable from the defined gene content of Tn*AbaR23* and the PCR-informed absence of a *sul1* gene elsewhere on the A424 chromosome. In contrast, the paradoxical changes in ciprofloxacin MIC values observed in DCO163 and DCO174 relative to that of A424 were entirely unexpected.

Tn*AbaR* transposon family. At this time, we have designated the ATCC17978 element as Tn*AbaR0* to reflect its presence in the earliest known *A. baumannii* isolate harboring such an element. Recently, an ~63-kb element which we designated Tn*AbaR20* was identified in *A. baumannii* strain HK302 and reported to be indistinguishable from Tn*AbaR3* by PCR mapping. Strain HK302 was originally isolated from the respiratory tract of a patient in an intensive care unit in Switzerland in 1977 (19). The discovery of Tn*AbaR20* emphasized the earlier than initially presumed origins of "well-armed" versions of these elements and the wide geographic dissemination of these entities, as its "PCR-identical twin," Tn*AbaR3*, was identified in AB0057, a strain originally isolated from the bloodstream of a patient in Washington, DC, only in 2004. However, consistent with the postulated plasticity of Tn*AbaR* elements, Tn*AbaR3* and Tn*AbaR20* represent the only two examples sharing an indistinguishable modular makeup (Fig. 3).

Contribution of Tn*AbaR23* to the resistance phenotype of *Acinetobacter baumannii* A424. Antibiotic susceptibility profiles of the wild-type strain A424 and its isogenic Tn*AbaR23*-minus mutants, DCO163 and DCO174, were determined (Table 2). Disc diffusion-based assays were performed for 16 antibiotics, and with the exception of sulfamethoxazole and trimethoprim-sulfamethoxazole, no major and/or consistent (matching results for both mutants) differences were observed between the results for wild-type strain A424 and its isogenic Tn*AbaR23*-minus mutants. Consistent with Tn*AbaR23* carrying two copies of *sul1*, both Tn*AbaR23*-minus mutants were significantly more sensitive to sulfamethoxazole than was the parent strain (Table 2). Zone of inhibition diameters for tetracycline also suggested that both mutants were less resistant to this agent than A424, although yet again DCO163 appeared to be even more susceptible than DCO174. In addition, both mutants exhibited slightly increased resistance to streptomycin, amikacin, and tobramycin and markedly increased resistance to gentamicin most probably as a result of acquisition of the gentamicin resistance-encoding *aacC1* cassette that was used to replace Tn*AbaR23*. Intriguingly, for the 10 antibiotics with mutant-to-mutant variation in zone of inhibition diameters, DCO163 consistently yielded larger zones than DCO174, except for rifampin where the measured discrepancy was very small (11.5 mm compared to 13.0 mm, respectively) and the reverse was true. As PFGE data suggested that DCO163 carries an additional undefined large deletion and as this mutant consistently exhibited increased susceptibility compared to DCO174, we postulated that DCO163 may display a growth defect relative to DCO174. However, growth curve analysis using LB medium and shaking incubation at 37°C failed to reveal any significant differences in growth kinetics between DCO163, DCO174, and the parent strain, A424 (Fig. 4A).

Etests were used to determine the MICs of a subset of these antibiotics (Table 2). As suggested through disc susceptibility analysis, the gentamicin MICs of both mutants were markedly elevated than that of wild-type strain A424 (16 μg/ml [DCO163] and 48 μg/ml [DCO174] compared to 0.75 μg/ml [A424]). Similarly, the amikacin MICs of the mutants were at least 4-fold that of

A424. The largest observed shifts corresponded to sulfamethoxazole MICs, with both mutants exhibiting MICs much less than 1/200th that of the wild-type strain (0.75 μg/ml [DCO163] and 4 μg/ml [DCO174] compared to >1,024 μg/ml [A424]) (Fig. 4B).

Given the roles of *gyrA* and *parC* point mutations in fluoroquinolone resistance in many bacterial species, we amplified and sequenced the quinolone resistance-determining regions (QRDRs) of these genes from strain A424 and the two Tn*AbaR23*-minus mutants. We had postulated that the markedly increased ciprofloxacin MIC values exhibited by DCO174 (>32 μg/ml) compared to A424 (4 μg/ml) or DCO163 (3 μg/ml) would be due to a distinguishing coincidental QRDR-associated mutation(s) in DCO174 (Fig. 4B). However, all three strains contained identical sequences over the available overlapping 289-bp and 326-bp segments wholly containing the QRDRs of *gyrA* and *parC*, respectively (see Fig. S2 in the supplemental material). Nevertheless, consistent with the elevated ciprofloxacin MIC levels of all three strains and previous reports on ciprofloxacin resistance-associated mutations in *A. baumannii* and other Gram-negative bacteria (34, 36), a mutation associated with the common Ser83Leu substitution in GyrA was detected. However, an accompanying Ser80Leu-associated mutation in *parC* was not observed, and no other *gyrA* or *parC* polymorphisms were detected within the QRDRs of these genes. A PCR screen for *qnrA*, a gene coding for plasmid-mediated ciprofloxacin resistance, was also negative for all three strains. Hence, the basis of the >8-fold increase in ciprofloxacin MIC of DCO174 relative to that of DCO163 and A424 remains elusive.

Summary. Despite the long list of Tn*AbaR* elements identified thus far, there have been no reports on the experimental characterization of these elements, though much has been inferred from sequence annotation information. Using a classical genetic strategy, we attempted to plug this gap by deleting Tn*AbaR23* from the clinically derived multidrug-resistant *A. baumannii* strain A424. In contrast to expectations, the two independently derived Tn*AbaR23*-minus mutants exhibited distinct but related PFGE profiles and discordant susceptibility patterns, despite both being conclusively shown to be isogenic with the wild-type parent strain. Most remarkably, the DCO174 mutant exhibited a >8-fold increase in its ciprofloxacin MIC, while the MIC of the second mutant, DCO163, closely resembled that of A424, despite all three strains sharing identical *gyrA* and *parC* QRDR sequences. Furthermore, as the NotI PFGE profile of DCO174 revealed no other incidental genomic changes, this mutant may well constitute a genuine single-mutation derivative of A424. If so, these data would suggest that loss of Tn*AbaR23* alone resulted in the markedly elevated ciprofloxacin MIC exhibited by DCO174. Alternatively, a cryptic secondary mutation, potentially affecting an efflux mechanism, may explain this finding. Experiments to define the basis of this intriguing phenomenon, potentially suggestive of a paradoxical role for Tn*AbaR23* in promoting sensitivity as opposed to resistance to ciprofloxacin, are under way. The nature of the additional genomic rearrangement and/or deletion in strain DCO163 is also being actively pursued, as the observed increased sensitivity to a broad range of antimicrobials without impairment of growth in antibiotic-free medium exhibited by DCO163 would suggest that this Tn*AbaR23*-minus mutant has lost a further yet-to-be-defined resistance-associated function. This study highlights the importance of experimental scrutiny of the function of Tn*AbaR* elements in *A. baumannii* and challenges the assumption that resistance phenotypes can be predicted from the genetic makeup of large resistance gene assemblages alone.

ACKNOWLEDGMENTS

We thank Nutan Sapkota, Shirley Tang, and Ansie Martin for technical assistance and are grateful to Kevin Towner for the donation of a large *A. baumannii* strain collection and to Alessandra Carratolli and Mark Adams and Robert Bonomo for strains ACICU and AB0057, respectively.

This work was funded by a British Society for Antimicrobial Chemotherapy (BSAC) research grant to K.R. H.-Y.O. was supported by the National Natural Science Foundation of China, the Program for New Century Excellent Talents in University, MOE, China (NCET-10-0572), and the Program for Chen Xing Scholars for Shanghai Jiaotong University. Genome sequencing was supported by a Medical Research Council grant (G0901717) to M.P. and C.C.

ADDENDUM IN PROOF

Since the submission of this manuscript, two further members of the Tn*AbaR* family have been described. AbaR21 is present in *A. baumannii* strain RUH875 (A297), a strain that has frequently served as a European clone I type strain (S. J. Nigro, V. Post, and R. M. Hall, J. Antimicrob. Chemother. 66:1928–1930). By contrast, AbaR22 is found in multidrug-resistant *A. baumannii* strain MDR-ZJ06, belonging to European clone II, which is widely disseminated in China (H. Zhou et al., Antimicrob. Agents Chemother. 55:4506–4512). Accordingly, we have named the presently reported element Tn*AbaR23*.

REFERENCES

1. **Adams MD, Chan ER, Molyneaux ND, Bonomo RA.** 2010. Genome-wide analysis of divergence of antibiotic resistance determinants in closely related isolates of *Acinetobacter baumannii.* Antimicrob. Agents Chemother. **54**:3569–3577.
2. **Adams MD, et al.** 2008. Comparative genome sequence analysis of multidrug-resistant *Acinetobacter baumannii.* J. Bacteriol. **190**:8053–8064.
3. **Andrews J.** 2010. BSAC methods for antimicrobial susceptibility testing. Version 9.1. March 2010. British Society for Antimicrobial Chemotherapy, Birmingham, United Kingdom. http://www.bsac.org.uk/Resources/BSAC/Version_9.1_March_2010_final.pdf.
4. **Bailey JK, Pinyon JL, Anantham S, Hall RM.** 2011. Distribution of the bla_{TEM} gene and bla_{TEM}-containing transposons in commensal *Escherichia coli.* J. Antimicrob. Chemother. **66**:745–751.
5. **Borremans B, Hobman JL, Provoost A, Brown NL, van Der Lelie D.** 2001. Cloning and functional analysis of the *pbr* lead resistance determinant of *Ralstonia metallidurans* CH34. J. Bacteriol. **183**:5651–5658.
6. **Branco R, Chung AP, Morais PV.** 2008. Sequencing and expression of two arsenic resistance operons with different functions in the highly arsenic-resistant strain *Ochrobactrum tritici* SCII24T. BMC Microbiol. **8**:95.
7. **Brocklehurst KR, Megit SJ, Morby AP.** 2003. Characterisation of CadR from *Pseudomonas aeruginosa*: a Cd(II)-responsive MerR homologue. Biochem. Biophys. Res. Commun. **308**:234–239.
8. **Cai J, Salmon K, DuBow MS.** 1998. A chromosomal *ars* operon homologue of *Pseudomonas aeruginosa* confers increased resistance to arsenic and antimony in *Escherichia coli.* Microbiology **144**:2705–2713.
9. **Chaudhuri RR, et al.** 2008. xBASE2: a comprehensive resource for comparative bacterial genomics. Nucleic Acids Res. **36**:D543–D546.
10. **Choi KH, Schweizer HP.** 2006. Mini-Tn*7* insertion in bacteria with single *att*Tn*7* sites: example *Pseudomonas aeruginosa.* Nat. Protoc. **1**:153–161.
11. **Damier-Piolle L, Magnet S, Brémont S, Lambert T, Courvalin P.** 2008. AdeIJK, a resistance-nodulation-cell division pump effluxing multiple antibiotics in *Acinetobacter baumannii.* Antimicrob. Agents Chemother. **52**:557–562.
12. **de Lorenzo V, Timmis KN.** 1994. Analysis and construction of stable phenotypes in gram-negative bacteria with Tn*5*- and Tn*10*-derived mini-transposons. Methods Enzymol. **235**:386–405.
13. **Dorsey CW, Tomaras AP, Actis LA.** 2002. Genetic and phenotypic analysis of *Acinetobacter baumannii* insertion derivatives generated with a transposome system. Appl. Environ. Microbiol. **68**:6353–6360.

14. **Fournier PE, et al.** 2006. Comparative genomics of multidrug resistance in *Acinetobacter baumannii.* PLoS Genet. **2**:e7.
15. **Harrison EM, et al.** 2010. Pathogenicity islands PAPI-1 and PAPI-2 contribute individually and synergistically to the virulence of *Pseudomonas aeruginosa* strain PA14. Infect. Immun. **78**:1437–1446.
16. **Herrero M, de Lorenzo V, Timmis KN.** 1990. Transposon vectors containing non-antibiotic resistance selection markers for cloning and stable chromosomal insertion of foreign genes in gram-negative bacteria. J. Bacteriol. **172**:6557–6567.
17. **Iacono M, et al.** 2008. Whole-genome pyrosequencing of an epidemic multidrug-resistant *Acinetobacter baumannii* strain belonging to the European clone II group. Antimicrob. Agents Chemother. **52**:2616–2625.
18. **Krizova L, Dijkshoorn L, Nemec A.** 2011. Diversity and evolution of AbaR genomic resistance islands in *Acinetobacter baumannii* strains of European clone I. Antimicrob. Agents Chemother. **55**:3201–3206.
19. **Krizova L, Nemec A.** 2010. A 63 kb genomic resistance island found in a multidrug-resistant *Acinetobacter baumannii* isolate of European clone I from 1977. J. Antimicrob. Chemother. **65**:1915–1918.
20. **Laponogov I, et al.** 2009. Structural insight into the quinolone-DNA cleavage complex of type IIA topoisomerases. Nat. Struct. Mol. Biol. **16**: 667–669.
21. **Lee SW, Glickmann E, Cooksey DA.** 2001. Chromosomal locus for cadmium resistance in *Pseudomonas putida* consisting of a cadmium-transporting ATPase and a MerR family response regulator. Appl. Environ. Microbiol. **67**:1437–1444.
22. **Madurga S, Sánchez-Céspedes J, Belda I, Vila J, Giralt E.** 2008. Mechanism of binding of fluoroquinolones to the quinolone resistance-determining region of DNA gyrase: towards an understanding of the molecular basis of quinolone resistance. ChemBioChem **9**:2081–2086.
23. **Muller D, et al.** 2007. A tale of two oxidation states: bacterial colonization of arsenic-rich environments. PLoS Genet. **3**:e53.
24. **Post V, Hall RM.** 2009. AbaR5, a large multiple-antibiotic resistance region found in *Acinetobacter baumannii.* Antimicrob. Agents Chemother. **53**:2667–2671.
25. **Post V, White PA, Hall RM.** 2010. Evolution of AbaR-type genomic resistance islands in multiply antibiotic-resistant *Acinetobacter baumannii.* J. Antimicrob. Chemother. **65**:1162–1170.
26. **Rajakumar K, Sasakawa C, Adler B.** 1997. Use of a novel approach, termed island probing, identifies the *Shigella flexneri she* pathogenicity island which encodes a homolog of the immunoglobulin A protease-like family of proteins. Infect. Immun. **65**:4606–4614.
27. **Rose A.** 2010. Tn*AbaR1*: a novel Tn*7*-related transposon in *Acinetobacter baumannii* that contributes to the accumulation and dissemination of large repertoires of resistance genes. Bioscience Horizons **3**:40–48.
28. **Rosenstein R, Peschel A, Wieland B, Götz F.** 1992. Expression and regulation of the antimonite, arsenite, and arsenate resistance operon of *Staphylococcus xylosus* plasmid pSX267. J. Bacteriol. **174**:3676–3683.
29. **Shaikh F, et al.** 2009. ATPase genes of diverse multidrug-resistant *Acinetobacter baumannii* isolates frequently harbour integrated DNA. J. Antimicrob. Chemother. **63**:260–264.
30. **Sone Y, Pan-Hou H, Nakamura R, Sakabe K, Kiyono M.** 2010. Role played by MerE and MerT in the transport of inorganic and organic mercury compounds in Gram-negative bacteria. J. Health Sci. **56**:123–127.
31. **Srinivasan VB, Rajamohan G, Gebreyes WA.** 2009. Role of AbeS, a novel efflux pump of the SMR family of transporters, in resistance to antimicrobial agents in *Acinetobacter baumannii.* Antimicrob. Agents Chemother. **53**:5312–5316.
32. **van Aartsen JJ, Rajakumar K.** 2011. An optimized method for suicide vector-based allelic exchange in *Klebsiella pneumoniae.* J. Microbiol. Methods **86**:313–319.
33. **Vila J, Martí S, Sánchez-Céspedes J.** 2007. Porins, efflux pumps and multidrug resistance in *Acinetobacter baumannii.* J. Antimicrob. Chemother. **59**:1210–1215.
34. **Vila J, Ruiz J, Goñi P, Jimenez de Anta T.** 1997. Quinolone-resistance mutations in the topoisomerase IV *parC* gene of *Acinetobacter baumannii.* J. Antimicrob. Chemother. **39**:757–762.
35. **Williams PA, Jones RM, Shaw LE.** 2002. A third transposable element, IS*Ppu12*, from the toluene-xylene catabolic plasmid pWW0 of *Pseudomonas putida* mt-2. J. Bacteriol. **184**:6572–6580.
36. **Wisplinghoff H, et al.** 2003. Mutations in *gyrA* and *parC* associated with resistance to fluoroquinolones in epidemiologically defined clinical strains of *Acinetobacter baumannii.* J. Antimicrob. Chemother. **51**:177–180.